IOVS Papers in Press. Published on June 24, 2009 as Manuscript iovs.09-3743

Development of Microelectrode Arrays for Artificial Retinal Implants using Liquid Crystal Polymers

Seung Woo Lee[1,3,4], Jong-Mo Seo[1,3,4], MD, Seungmin Ha[2,3,4], MD, Eui Tae Kim[1,3,4], Hum Chung[2,3,4], MD and Sung June Kim[1,3,4], PhD

[1]School of Electrical Engineering and Computer Science
[2]Department of Ophthalmology, Seoul National University College of Medicine and
[3]Seoul Artificial Eye Center
[4]Nano Bioelectronics & Systems Research Center (NBS-ERC)
Seoul National University, Seoul, Korea

Corresponding Author:

Sung June Kim, PhD

Address: Bldg. 301 Room# 1006, Seoul National University, San 56-1, Shinlim-dong, Gwanak-gu, Seoul, 151-742, Korea

Mail: kimsj@snu.ac.kr

Tel: +82-2-880-1812

Fax: +82-2-882-4158

Abstract

Purpose: To develop a liquid crystal polymer (LCP) based, long-term implantable, retinal stimulation microelectrode array using a novel fabrication method.

Methods: The fabrication process used laser micromachining and customized thermal-press bonding to produce LCP based microelectrode arrays. To evaluate the fabrication process and the resulting electrode arrays, *in vitro* reliability tests and *in vivo* animal experiments were performed. The *in vitro* tests consisted of electrode site impedance recording and electrode inter-layer adhesion monitoring during accelerated soak tests. For *in vivo* testing, the fabricated electrode arrays were implanted in the suprachoroidal space of rabbit eyes. Optical coherence tomography (OCT) and electrically evoked cortical potentials (EECPs) were used to determine long-term biocompatibility and functionality of the implant.

Results: The fabricated structure had a smooth, rounded edge profile and exhibited moderate flexibility, which are advantageous features for safe implantation without guide tools. Following accelerated soak tests at 75°C in phosphate buffered saline, the electrode sites showed no degradation and the inter-layer adhesion of the structure showed acceptable stability for more than 2 months. The electrode arrays were safely

implanted in the suprachoroidal space of rabbit eyes, and EECP waveforms were recorded. Over a 3-month postoperative period, no choroioretinal inflammation or structural deformities were observed by OCT and histological examination.

Conclusions: LCP based flexible microelectrode arrays can be successfully applied as retinal prostheses. The results demonstrate that such electrode arrays are safe, biocompatible, mechanically stable, and can be effective as part of a chronic retinal implant system.

Keywords: Liquid crystal polymer (LCP), microelectrode array, retinal prosthesis, blister test, optical coherence tomography, electrically evoked cortical potentials.

1. Introduction

Electrical stimulation of the remaining retinal neurons of patients with degenerated photoreceptors has been studied as a potential method for the provision of artificial vision. To transfer and control such electrical stimulation, several research groups have developed polymer-based flexible microelectrode arrays.[1-4] To date, several polymer materials, including polyimide, parylene, and silicone, have been used as substrate materials for retinal stimulation electrode arrays. These polymers are thin, flexible, and biocompatible, *i.e*., suitable characteristics for minimally invasive retinal electrode arrays. Although retinal stimulation electrode arrays fabricated on these polymers have been reported to be safe and effective in previous *in vivo* and *in vitro* studies, including animal and human trials,[1-4] there is controversy about the long-term reliability of the polymers. These concerns are related to the polymers' relatively high water absorption and unstable interfacial adhesion properties in aqueous environments.[5-7]

Liquid crystal polymers (LCPs) are flexible, mechanically stable, and biocompatible materials that have very low moisture absorption (<0.04%) when compared to polyimide, parylene, and silicone.[8-14] LCPs exhibit excellent barrier

properties against various chemicals and can be thermally bonded to each other without adhesives.[8-15] Because of their high reliability under harsh environmental conditions, LCPs have been investigated as long-term reliable substrate materials for high performance printed circuit boards,[8,15] micro-electromechanical system sensors,[10] and neural prostheses.[11,12]

In this paper, we report the development of a novel retinal stimulation microelectrode array using LCPs and report on the electrode array's performance during *in vitro* and *in vivo* experiments. A simplified fabrication process for such LCP based microelectrode arrays is also introduced.

2. Materials and Methods

2.1. Fabrication process

The fabrication process, which uses laser micromachining and customized thermal-press bonding, is shown in Fig. 1(a). Briefly, a 25 µm thick low melting temperature (280°C) LCP (Vecstar FA-25N, Kuraray Co., Ltd., Tokyo, Japan) film and a 25 µm thick high melting temperature (315°C) LCP (Vecstar OCL-25N, Kuraray) film were cut into 100 mm diameter circles using a UV laser drilling system (Flex5330,

Electro Scientific Industries, Inc., Portland, OR, USA) to create a substrate and a cover, respectively. In the laser machining process, alignment marks were engraved on both the substrate and cover pieces, and electrode site windows (500 µm diameter for the stimulation sites and 1400 µm diameter for a reference site) were created in the cover. The machined substrate LCP was attached to a similar sized silicon wafer, using photoresist (AZ4620, AZ Electronic Materials, Luxembourg, Luxembourg) as an adhesive, before undergoing additional processes that required planar surface properties.[10-12, 14]

Subsequently, titanium (100 nm thick), gold (400 nm thick), and/or titanium (100 nm thick) layers were consecutively deposited on the LCP substrate by a sputter machine (ALPS-C03, Alpha Plus Co., Ltd., Pohang, Korea). The Ti layers form biocompatible adhesion layers between the electrode site metals (Au, Pt and IrOx) and the LCP films.[11,12,14] Prior to metal patterning, photoresist (AZ1512, AZ Electronic Materials) was spin-coated on the metal-bearing substrate. Photolithography was then performed using a mask aligner machine (MA6/BA6, SUSS MicroTec, Garching, Germany). Subsequently, the metal microelectrode patterns were created by a conventional wet etching process.

After the patterning process, the substrate was released from the silicon wafer

using acetone. The cover was then positioned on the substrate using the alignment marks, and the pair placed into a custom aluminum mold, comprising 100 mm diameter planar plates and four alignment pins. Thermal-press bonding[15] was performed at 300 psi (2.1 MPa) and 285°C for 45 min using a heated press (Model CH, Press no. 4386, Carver, Inc., Wabash, IN, USA). Subsequently, the laminated structure was cut into the final microelectrode array shape (Fig. 1(b)) using the aforementioned UV laser machining system (Electro Scientific Industries).

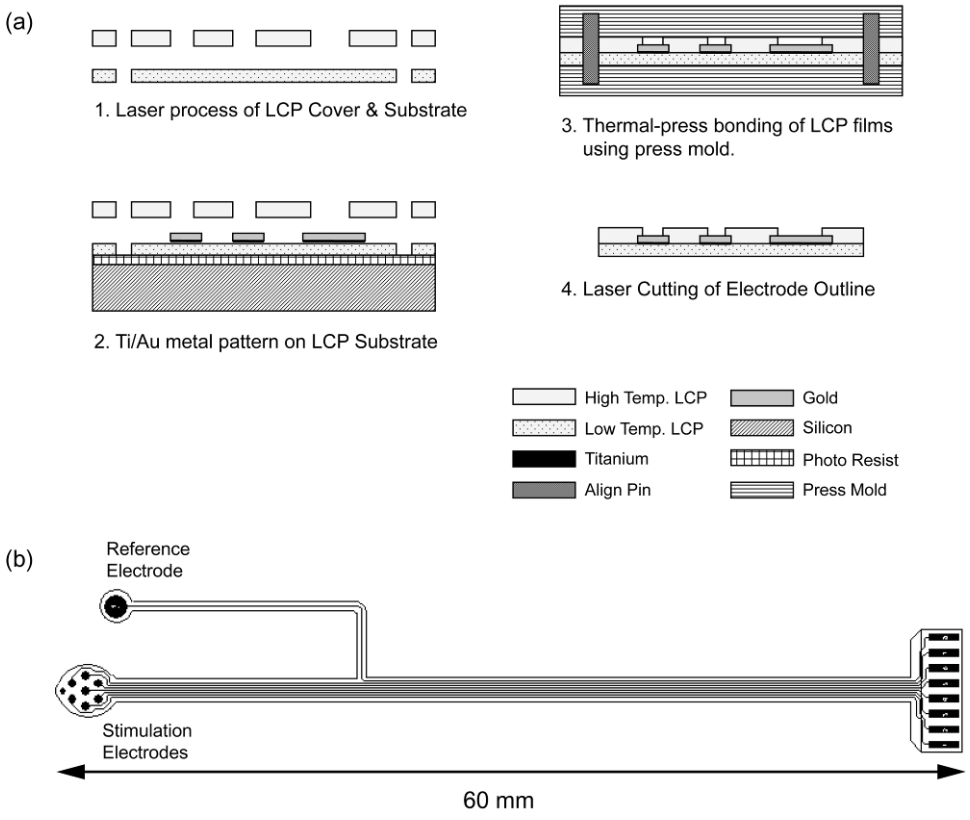

Figure 1. (a) Representative schematic of LCP based microelectrode array fabrication

process. Laser machining was utilized for patterning the substrate and cover films, and for cutting the electrode array outlines. Thermal-press bonding was performed to create the LCP multi-layered structure. Total thickness of the structure is controllable from 50 to 75 µm with a 25 µm-thick additional substrate. (b) Schematic diagram of LCP based retinal electrode array. This structure has 7 stimulation sites and 1 reference site. The diameters of the stimulation site and reference site windows are 500 µm and 1400 µm, respectively.

2.2. *In vitro* Reliability Tests

To evaluate the reliability of polymer based electrode arrays, various testing methods have been used.[6,7] For electrical reliability testing, electrical leakage current measurement between adjacent leads has been used.[7] For mechanical reliability testing, inter-layer adhesion strengths have been measured.[6] We considered both of these testing methods to evaluate the overall reliability of the fabricated microelectrode arrays; however, in this paper we focused on tests that indicate long-term structural reliability.

To assess the long-term structural reliability of the LCP based electrode arrays within a relatively short time, electrode site impedance and adhesion strength of the LCP multi-layered structures were monitored during *in vitro* accelerated (75°C) and

non-accelerated (37°C) soak tests. The soak tests were performed in phosphate-buffered saline (PBS) solution (Gibco #10010, Invitrogen Life Technologies, Carlsbad, CA, USA). Monitoring of electrode site impedance provided information on electrical connectivity and the exposed site metal status. We selected 5 sites (stimulation channels 1, 2, 3, 4 and the reference electrode; Fig. 2(b)) among the 8 available sites, and during the soak tests regularly measured their impedance (magnitude) at 1 kHz 5 mV amplitude sine waveform using an impedance analyzer (IM6e, Zahner-Elektrik, Kronach, Germany), as shown in Fig. 2(a).

Monitoring of adhesion strength provided information about the durability of the multi-layered structure. The adhesion strength was measured using a customized blister test. To compare the results, previously reported data of polyimide adhesion strengths, comprising polyimide/polyimide and titanium/polyimide interfaces, were used. (Lee SW, et al. *IOVS* 2007;136:ARVO E-Abstract 664). Fig. 2(c) shows a cross section of the structure of the blister test samples, which were fabricated in a similar manner as the structure of the aforementioned LCP based microelectrode arrays. The tested structures consisted of bonded high and low melting temperature LCPs with metal at the LCP interface. As a Ti layer was used as the adhesion layer in the Au microelectrode arrays, we focused on testing LCP/LCP and Ti/LCP interface adhesions.

The LCP/LCP sample consisted of a high melting temperature LCP substrate, a low melting temperature LCP inter-layer and a high melting temperature LCP cover (Fig. 2(c)). On the inter-layer and the cover, Ø 4 mm and Ø 2 mm holes, respectively, were created by UV laser machining (Electro Scientific Industries). The Ti/LCP sample consisted of the same LCP/LCP structure, but with a Ti (100 nm) layer deposited on the LCP cover.

A conceptual diagram of the customized blister test is presented in Fig. 2(e). Subsequent to soak testing, adhesion strength was measured as the critical pressure (MPa) which can initiate crack propagation between the films. To perform the blister test, the cover side of the sample is attached to a metal holder, which had a Ø 4 mm hole, using an acrylate adhesive (Uni-401, Dong Sung Uni-Tech, Pocheon, Korea) with a bonding strength of 200 kg/cm^2 (19.6 MPa). The metal holder was positioned in the apparatus (Fig. 2(f)), and pressure was applied to the sample using N_2 gas supplied through the Ø 4 mm hole in the metal holder. The applied pressure was controlled by a precision regulator (Harris Products Group, Mason, OH, USA). The maximum available pressure was 1.1 MPa. During the crack initiation test, changes in blister diameter and height were monitored with two charge coupled device (CCD) cameras (MTV-7266ND, Mintron Enterprise Co., Taipei, Taiwan).

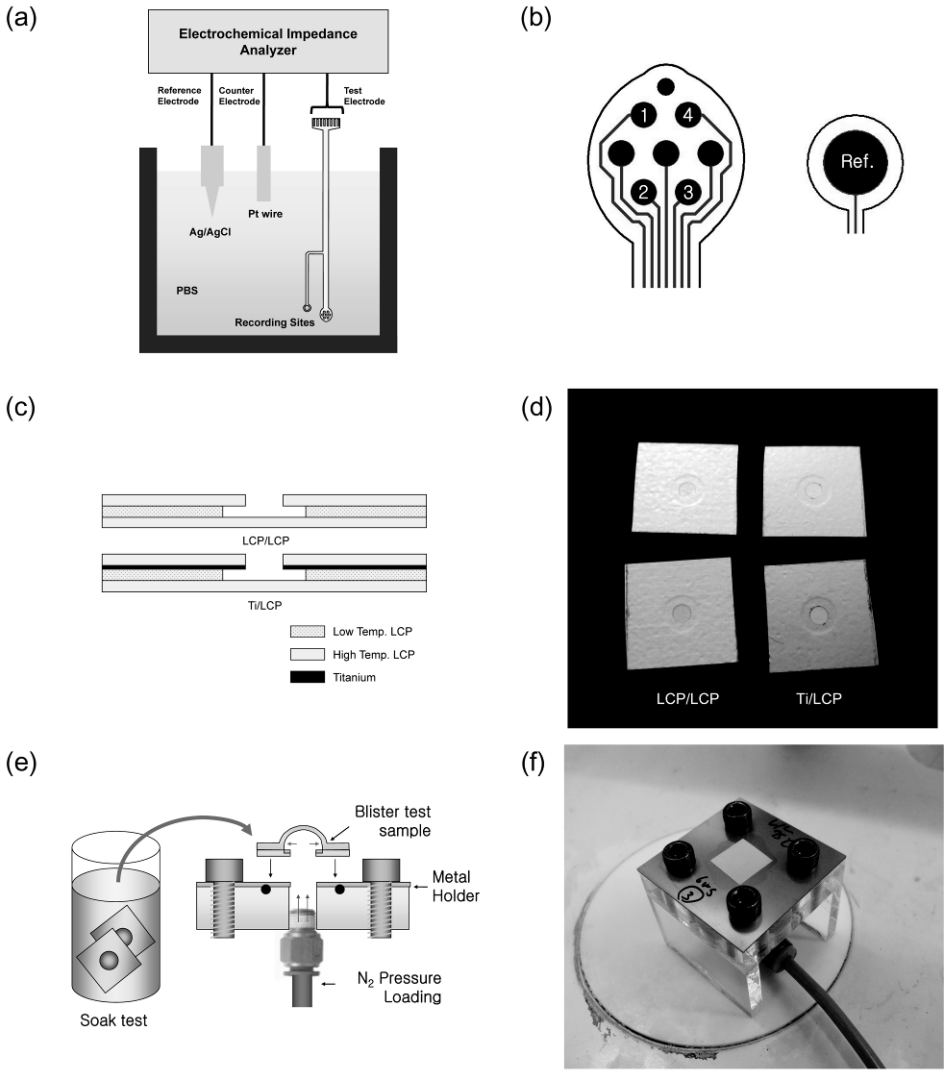

Figure 2. *In vitro* reliability tests: (a) schematic diagram of electrode site impedance measurement apparatus, (b) schematic diagram of electrode site arrangement showing channel numbers 1-4 and the reference electrode, (c) cross sectional diagram showing layers in the blister test samples for determination of adhesion strength between LCP/LCP and Ti/LCP interfaces, (d) photographs of samples for blister testing, (e)

conceptual diagram of soak and blister testing process, and (f) photograph of blister test apparatus.

2.3. *In vivo* Animal Experiments

To demonstrate the application feasibility of the fabricated electrode arrays, *in vivo* animal experiments were performed using New Zealand White rabbits. All procedures conformed to the Association for Research in Vision and Ophthalmology (ARVO) Statement for the Use of Animals in Ophthalmic and Vision Research. General anesthesia was induced by intramuscular injection of tiletamine/zolazepam (Zoletil, Virbac Laboratories, Carros, France) and xylazine (Rompun, Bayer AG, Leverkusen, Germany) in a 1:1 mixture. The rate of injection was 0.6 mL/kg. A conjunctival incision was done along the limbus at the 1 o'clock position, and a 4 mm scleral incision parallel to the limbus was made with a crescent knife (Sharptome 74-1010, Surgical Specialties Co., Reading, PA, USA). The fabricated LCP microelectrode arrays were implanted into the suprachoroidal space under panfunduscopic examination assisted by an indirect contact lens (Quad Pediatric, Volk Optical Inc., Mentor, OH, USA) in order to locate the electrode array under the visual streak adjacent to the optic disc. The external part of the electrode array was stabilized by placement over the sclera and under the extraocular

muscles, similar to the fixation achieved in circumferential scleral buckling.

After implantation, electrophysiological tests were performed to determine electrode array functionality. Biphasic current stimulation pulses were applied to the rabbit's retina through the electrode arrays and electrically evoked cortical potentials (EECPs) were simultaneously recorded from a stainless needle electrode (Rochester Electro-Medical Inc., Tampa, FL, USA) in the visual cortex using a multi-channel neuro-physiological workstation (Tucker-Davis Technologies, Alachua, FL, USA). These EECPs recordings were acute and performed using a previously reported system.[18] Briefly, the recording electrode (a single needle electrode) was inserted into a fine hole drilled in the skull (without craniotomy). The hole was located 6 mm anterior and 4 mm contralateral to lambda, an area previously reported as a good position for EECPs recordings.[18] The reference electrode (a single needle electrode) was inserted into a hole located 20 mm anterior to the lambda. The counter electrode (ground electrode) was inserted in the ipsilateral ear.

For the long-term biocompatibility and stability evaluation, the LCP microelectrode arrays were implanted in five rabbit eyes and monitored using optical coherence tomography (OCT; Cirrus OCT, Carl Zeiss, Dublin, CA, USA.) for 3 months. During the test period, fundus examinations were performed to evaluate any

inflammatory changes or other complications in vitreous and retinal areas. After 4 months, two rabbits were sacrificed and their eyes were enucleated to determine cataract or other morphological changes in the eye. Histological changes in the retina were evaluated using light microscopy and a hematoxylin-eosin stain.

3. Results

3.1. Fabrication Results

The LCP based microelectrode arrays were fabricated using the aforementioned process and their morphologies were examined with a field emission scanning electron microscope (FE-SEM; S-4800 UHR FE-SEM, Hitachi High-Technologies, Tokyo, Japan). Fig. 3 shows the array outline, the Au electrode site windows, the LCP cover surface, and the overall structure. The FE-SEM images indicate that laser cutting produced a smooth, rounded edge on the array outline (Fig. 3(a), (b)). The Au electrode site/LCP window edges were smooth, distinct, and without misalignment (Fig. 3(c), (d)). In addition, no burrs and residues were observed in the surrounding areas.

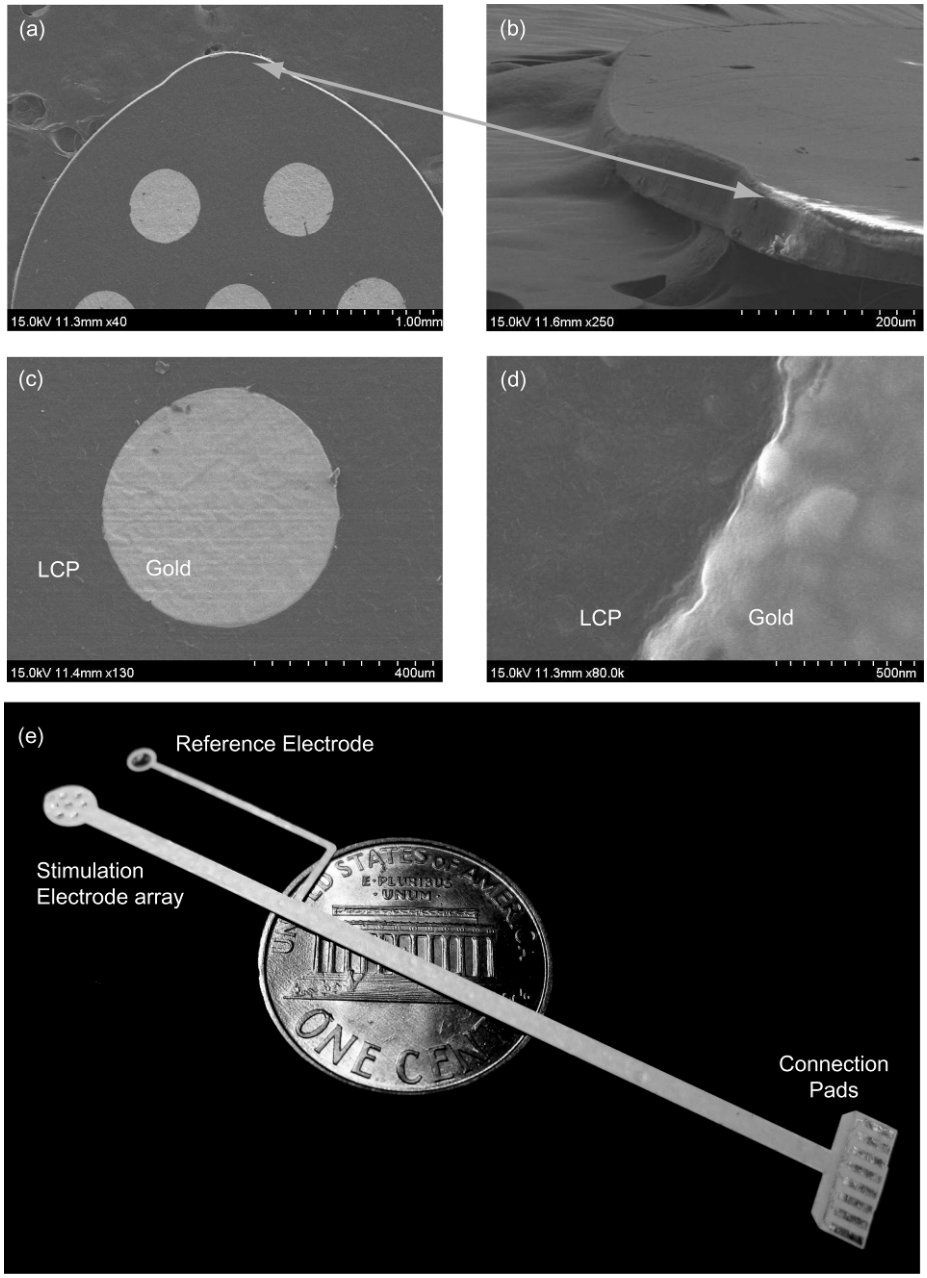

Figure 3. Photographs of LCP based Au microelectrode array: (a) FE-SEM image of microelectrode array (Top view) and (b) oblique view of a portion of the array edge, (c) 500 µm diameter Au site and (d) a portion of the Au site window edge. Laser machined site windows and structure outlines exhibited clear, smooth, and rounded edge features.

(e) a photograph of the overall structure.

3.2. *In vitro* Reliability Tests

The site impedance of the fabricated microelectrode array was monitored during 9 week soak tests at 37°C and 75°C. For the first week, impedance was measured daily, and in the remaining weeks impedance sampling was performed once a week. As shown in Fig. 4, the electrode impedance showed initial drop before reaching steady values. The impedance from the 75°C soak stabilized more quickly than that from the 37°C soak. Such decrease of impedance has been observed by other groups who employed various types of neural probes[19-22] and the change has been attributed to metal-fluid interface equilibration.[21] This change could have been accelerated at higher temperature. After the stabilization period, the impedance of each of the electrode sites was maintained over the 8 weeks and there was no marked differences between the soak test results from the two soak temperatures (Fig. 4). These results showed that the electrical connections of all test channels were sustained, and indicated that the exposed electrode sites on LCP were well preserved during the test period.

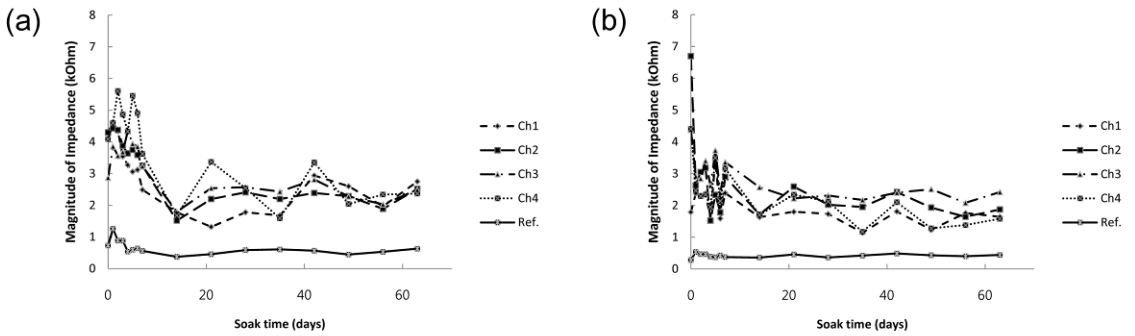

Figure 4. Electrode site impedance monitoring data: (a) magnitude of impedance of Au electrodes on LCP under 37ºC PBS soak test, and (b) magnitude of impedance at 75ºC. The electrode impedance showed initial drop before reaching steady values. The impedance from the 75°C soak stabilized more quickly than that from the 37°C soak. After the stabilization period, the impedance of each of the electrode sites was maintained over the 8 weeks and there was no marked differences between the soak test results from the two soak temperatures.

The blister test results (Fig. 5) showed that the LCP/LCP and Ti/LCP adhesions were strong and reliable in comparison to polyimide/polyimide (PI/PI) and titanium/polyimide (Ti/PI) during 8 week soak tests. Initial adhesion strength data revealed that the LCP/LCP (1.0897±0.0138 MPa) and Ti/LCP (1.0097±0.0807 MPa) interfaces were stronger than the PI/PI (0.9862±0.0712 MPa) and Ti/PI (0.4414±0.0253 MPa) interfaces (Fig. 5(a)). In non-accelerated soak tests at 37°C the LCP/LCP and

Ti/LCP interfaces showed no change in adhesion strengths (Fig. 5(b)) during the 8 week test period. In the accelerated soak tests at 75°C, during the same test period the PI/PI and Ti/PI adhesion strengths markedly decreased by 58.7% and 63%, respectively (Lee SW, et al. *IOVS* 2007;136:ARVO E-Abstract 664), but the LCP/LCP and Ti/LCP adhesion strengths decreased by only 8.1% and 11.5%, respectively.

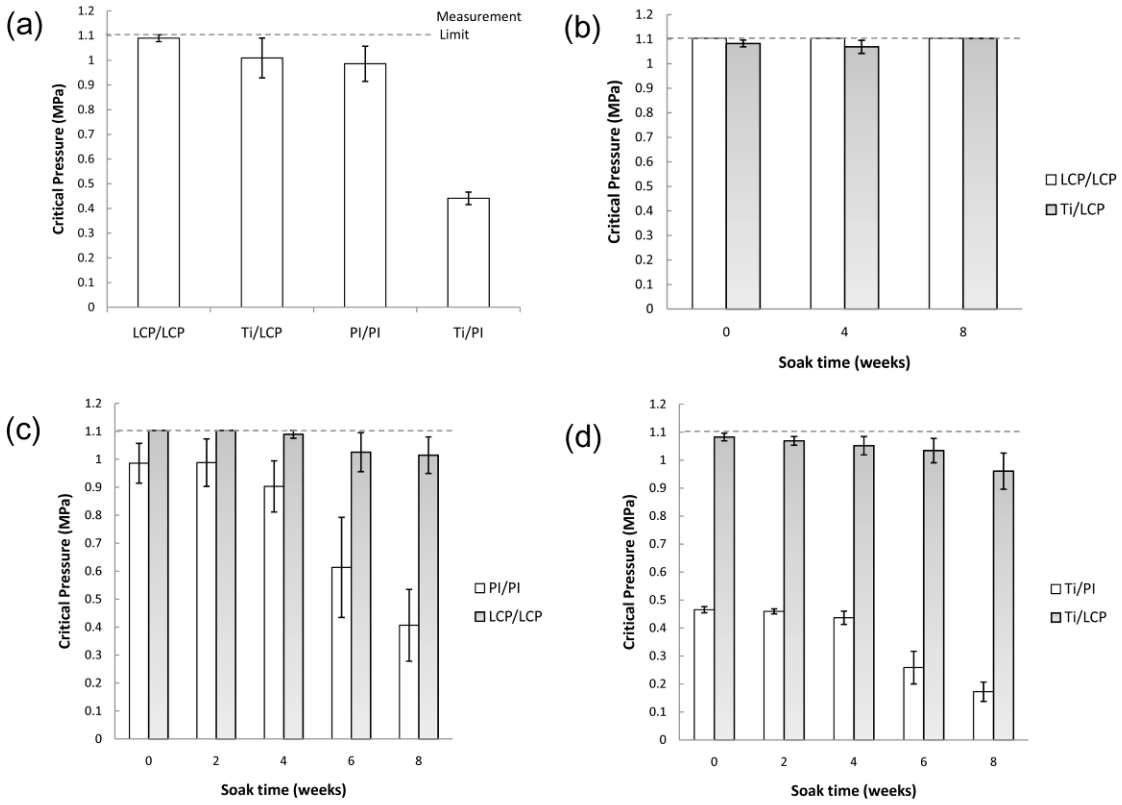

Figure 5. Blister test results: (a) initial adhesion strengths without soaking, (b) adhesion of LCP/LCP and Ti/LCP interfaces under 37ºC PBS soak test, (c) adhesion of LCP/LCP and PI/PI interfaces under 75ºC PBS soak test, and (d) adhesion of Ti/LCP and Ti/PI

interfaces under 75ºC PBS soak test. The measurement limit (1.1 MPa) was the upper limit of applied pressure in the test apparatus. Error bars represent ±1 standard error (N = 5). The data show that the LCP/LCP and Ti/LCP interfaces were stronger and more reliable than the PI/PI and Ti/PI interfaces during the 8 week soak test.

3.3. *In vivo* Animal Experiments

The fabricated microelectrode arrays were successfully implanted in the supra-choroidal space of the rabbit eyes. During insertion, no guide tools were needed because the fabricated structure exhibited an adequate amount of flexibility. The stimulation sites were successfully located near the retina's visual streak, and the reference site was located at the outer wall of the sclera.

Acute *in vivo* electrical stimulation experiments were performed to record the EECPs from the rabbit visual cortex. Cathodic-first biphasic current pulses of 0–100 μA amplitude, 1 ms duration, and 1 Hz period with 1 ms inter-phase delay were applied between the four stimulation sites and the reference site (Fig. 2(b)), and EECPs waveforms were simultaneously recorded (Fig. 6(a)). The waveforms exhibited the typical characteristics of EECPs, which have discernable negative and positive waves following the stimulus artifact components. The threshold current amplitude was

estimated at about 40 μA under four-channel simultaneous stimulation (40 μA × 4 channels simultaneously) and the threshold charge density was calculated as 20.4 $\mu C/cm^2$ (500 μm diameter). Because the stimulus artifact (Fig. 6(a)) component might have distorted and/or reduced the amplitude of the negative wave (N1 in Fig. 6(a)), the implicit time of the first negative peak was estimated at <16 ms. The first positive peak (P1 in Fig. 6(a)) was clearly observed and its implicit time was 26 ms. This relatively slow wave is similar to those observed in previous suprachoroidal stimulations[17,18] and clearly different from that resulting from a stimulus artifact. In addition, the first positive peak (P1) amplitude had a nearly linear relationship with the stimulation amplitude (Fig. 6(b)).

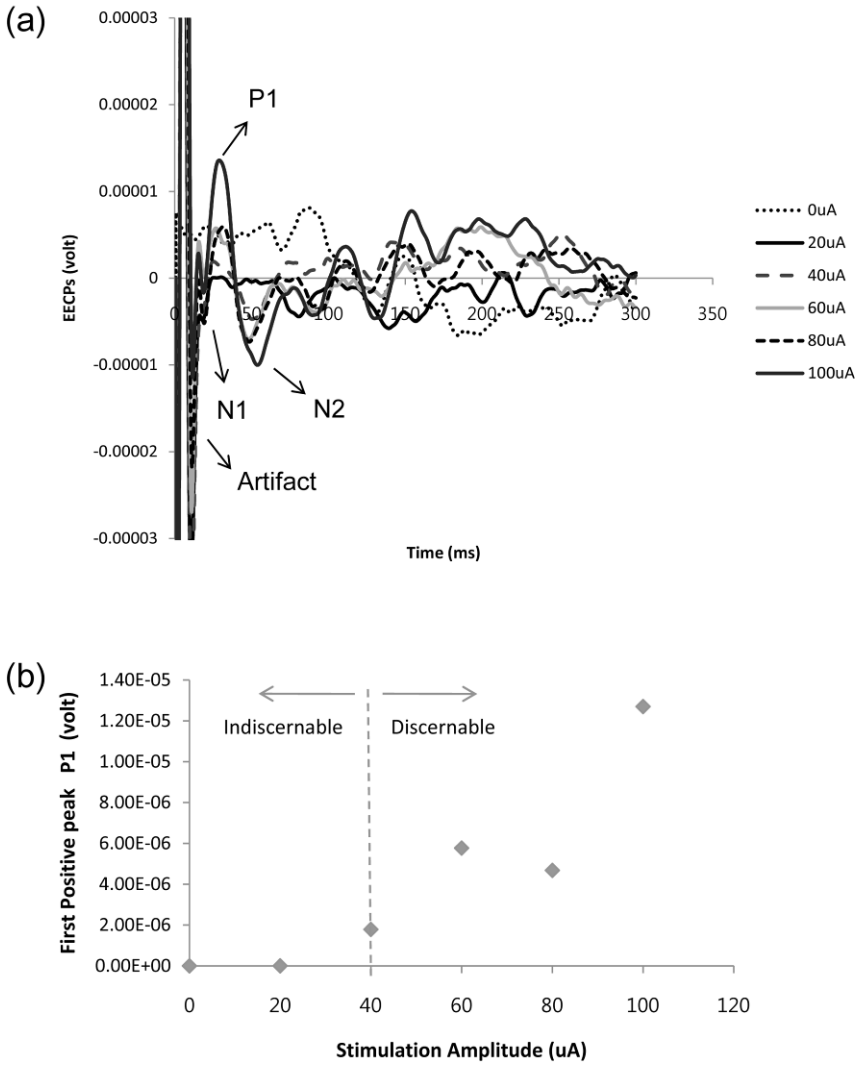

Figure 6. EECPs recording: (a) Representative EECP waveforms measured in visual cortex of a rabbit, (b) relationship between stimulation intensity and the first positive peak amplitude. The first positive peak (P1) was clearly observed and its implicit time was 26 ms. And, P1 had a nearly linear relationship with the stimulation amplitude.

The implanted electrode arrays were monitored by fundus observation and OCT

for 3 months. Subsequently, after 4 months, histological examinations were performed, and FE-SEM images were taken to evaluate array condition. The representative OCT images in Figs. 7(a) and (b) showed that the retina structures containing the LCP based retinal electrode arrays were well preserved during the postoperative 3-month period without observation of any choroioretinal inflammation or structural deformities. Moreover, the fundus images in Figs. 7(c) and (d) showed that the implanted arrays had not migrated, induced haziness, or resulted in vitreous inflammation. The histological examinations (Fig. 7(e)) revealed no evidence of retinal neural cell loss or inflammation around the space where the arrays were implanted after 4 months. The FE-SEM image of the explanted array (Fig. 7(f)) showed no sign of degradation such as delamination of sites or site windows.

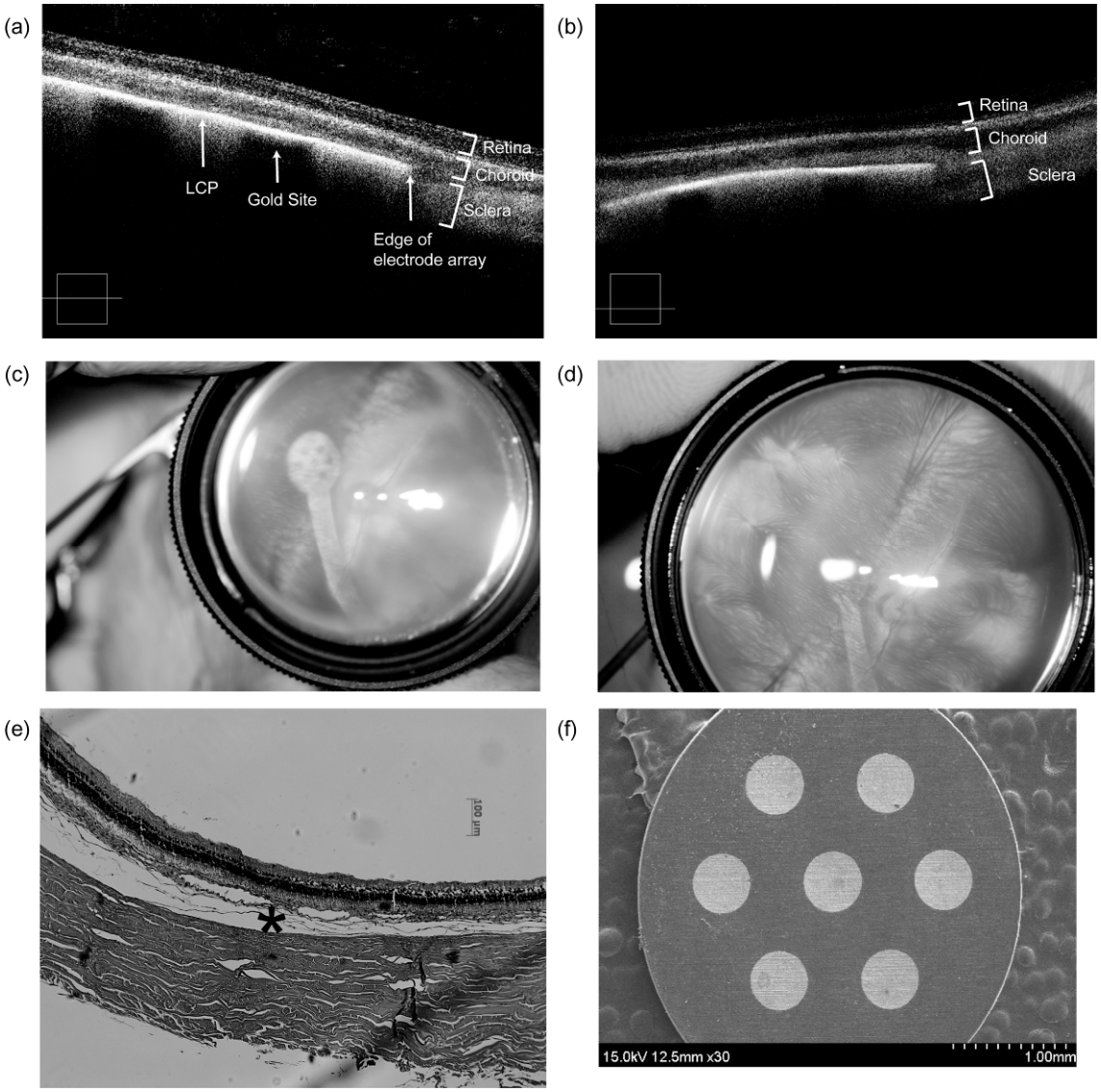

Figure 7. Suprachoroidally implanted microelectrode array in the rabbit eye: (a) OCT image – 2 weeks post-operation, (b) OCT image - 12 weeks post-operation. (c) fundus image - immediately after operation, (d) fundus image 7 weeks post-operation, (e) histology of the retina – 16 weeks post operation (* indicates the space where the microelectrode array was implanted), (f) FE-SEM image of the microelectrode array explanted after 16 weeks. The retina structures with LCP based microelectrode array

were well preserved at the end of the 4 month period. No migration or deformation of the implanted array was found.

4. Discussion

4.1. Characterization of the fabrication process

The LCP fabrication process is different from existing polymer fabrication processes for polyimide and parylene. First, LCP is a thermoplastic polymer that is supplied as a thin, film-type product[14]. Therefore, no spin-coating and curing processes, which are generally used in thermosetting polymer fabrication, are needed to fabricate the substrate and the insulation layer. Moreover, LCP films can be thermally bonded to other LCP films without adhesives[10,12,13,15]; accordingly, seamless, monolithic encapsulation of microelectrode arrays is available.

Although LCPs are a physically stable and chemically inert material, they has disadvantages in their compatibility with conventional photolithography alignment and plasma dry etching methods. Conventionally, alignment is performed using metal patterned alignment marks on the substrate. However, such marks cannot be observed through an LCP film due to its opacity; thus, a conventional alignment process is not

suitable. Moreover, plasma dry etching of LCP results in a slow etching rate and irregular surface morphologies and therefore requires additional time to create smooth site windows and electrode array outlines. To overcome these difficulties, modifications to conventional fabrication procedures were needed.

In our work, laser micromachining was fully exploited for improving fabrication productivity. Laser drilled alignment marks were useful for precise alignment, and laser machining produced a fast etching rate with high flexibility. Although laser machining is a serial process, often disadvantageous to batch fabrication, it is suitable for simplified fabrication of LCP material.

4.2. Long-term reliability test methodology

A potential source of failure of polymer based electrode arrays is the possibility of high electrical leakage between channels due to water absorption and unstable interfaces. Such failure can occur when the array structure experiences high-humidity environments[5-7]. Because of moisture and ion influences, the adhesion strength of the electrode array's inter-layer can decrease, allowing electrical leakage through the damaged interface. Once leakage paths are created, inter-electrode cross-talk increases significantly and eventually the electrode arrays would lose stimulation or recording

selectivity.

In this study, for detection and analysis of such potential failures within a shortened period, we used accelerated soak tests. At temperatures higher than 37°C, the structure degradation process caused by moisture and ion influences may be accelerated[5-7]. During our 75°C accelerated soak tests, we monitored electrode site impedance and inter-layer adhesion strength to evaluate site and inter-layer reliabilities. However, those measures could not provide direct information about the electrical reliability such as cross-channel leakage. Therefore, we are currently performing experiments to measure electrical current leakage through LCP interfaces using customized multi-interdigitated electrodes (MIDEs). Preliminary results have shown minute (2.1~38 pA) interface leakage currents during a 1 week experiment at 75°C under 5 V DC bias voltage (data not shown). These experimental results support the site impedance and inter-layer strength reported here.

Although accelerated soak tests are convenient for fast analysis of possible failure mechanisms, some potential pitfalls should be considered. First of all, the test temperature has to be carefully selected to avoid material transition or decomposition which may not occur under normal temperature conditions. In addition, unknown repair or stabilization processes can occur under accelerated conditions.[6,7] These are why we

performed the soak tests at both temperatures 37°C and 75°C.

4.3. Conclusion and future work

In this study, we fabricated and tested a prototype LCP based Au microelectrode array. Although Au was used, other site materials such as Pt and IrOx could be applied to our fabrication process using well established sputtering methods. Similar studies into their long-term reliabilities with LCP substrates will be reported in the future.

In vitro accelerated reliability tests showed that such LCP based microelectrode arrays have excellent stabilities in a high-humidity environment. Furthermore, even under high temperature (75°C) PBS soak tests, Au site conditions and inter-layer adhesion strengths of the electrode arrays showed no degradation for periods of 9 weeks and 8 weeks, respectively. These results can be explained by the very low moisture absorption (<0.04%) and thermal bondable interface characteristics of LCPs.

The feasibility and long-term biocompatibility of LCP based microelectrode arrays were examined by *in vivo* animal experiments including EECPs recording, OCT imaging, and histological examination. Typical EECP waveforms were recorded, and OCT images and histology after 3 months of implantation showed good biocompatibility.

Acknowledgements

This paper was supported by the Korea Science and Engineering Foundation (KOSEF) through the Nano Bioelectronics and Systems Research Center (NBS-ERC) at Seoul National University, and by a grant from the Korea Health 21 R&D Project (A050251), Ministry of Health & Welfare, Republic of Korea.

References

[1] Humayun MS, Weiland JD, Fujii GY, et al. Visual perception in a blind subject with a chronic microelectronic retinal prosthesis. *Vision Res*. 2003;43:2573-2581.

[2] Walter P, Kisvárday ZF, Görtz M, et al. Cortical Activation Via an Implanted Wireless Retinal Prosthesis. *Invest Ophthalmol Vis Sci*. 2005;46:1780-1784.

[3] Seo JM, Kim SJ, Chung H, et al. Biocompatibility of polyimide microelectrode array for retinal stimulation. *J Mater Sci Eng C*. 2004;24:185-189.

[4] Sachs HG, Schanze T. Wilms M, et al. Subretinal implantation and testing of polyimide film electrodes in cats. *Graefe's Arch Clin Exp Ophthalmol*. 2005;243:464-

468.

[5] DEIASI R, Russell J. Aqueous Degradation of Polyimides. *J Appl Polym Sci*. 1971;15:2965-2974.

[6] Murray S, Hillman C, Pecht M. Environmental Aging and Deadhesion of Polyimide Dielectric Films. *J Electron Packag*. 2004;126:390-397.

[7] Edell DJ. Insulating Biomaterials N01-NS-2-2347. *NINDS Quarterly Progress Report*. 2002.

[8] Jayaraj K, Farrell B, Liquid crystal polymers and their role in electronic packaging. *Adv Microelectron*. 1998;25:15-18.

[9] Culbertson EC, A New Laminate Material for High Performance PCBs: Liquid Crystal Polymer Copper Clad Films. *Electronic Components and Technology Conference Proceedings.* 1995;1995:520-523.

[10] Wang X, Engel J, Liu C, Liquid crystal polymer (LCP) for MEMS: process and applications. *J Micromech Microeng.* 2003;13:628-633.

[11] Lee CJ, Oh SJ, Song JK, et al. Neural signal recording using microelectrode arrays fabricated on liquid crystal polymer material, *J Mater Sci Eng C.* 2004;24:265-268.

[12] Keesara VV, Durand DM, Zorman CA. Fabrication and Characterization of Flexible, Microfabricated Neural Electrode Arrays Made from Liquid Crystal Polymer

and Polynorbornene. *Materials Research Society Symposium Proceedings 926E*, 2006: 0926-CC06-04.

[13] Thompson DC, Tentzeris MM, Papapolymerou J. Packaging of MMICs in Multilayer LCP Substrates, *IEEE Microw Wireless Compon Lett.* 2006;16:410-412.

[14] Dean RN, Weller J, Bozack MJ, et al. Realization of Ultra Fine Pitch Traces on LCP Substrates, *IEEE Trans Compon Packag Tech.* 2008;31:315-321.

[15] Rogers Corporation, R/flex 3000 Series Liquid Crystal Polymer Circuit Materials Fabrication Guidelines, (2005) Available online at http://www.rogerscorporation.com

[16] Wang C. Measurement of Interfacial Strength from the Blister Test. *J Appl Polym Sci*. 1999;73:1899-1912.

[17] Sakaguchi H, Fujikado T, Fang X, et al. Transretinal Electrical Stimulation with a Suprachoroidal Multichannel Electrode in Rabbit Eyes. *Jpn J Ophthalmol*. 2004;48:256-261.

[18] Kim ET, Seo JM, Woo SJ, et al. Fabrication of Pillar Shaped Electrode Arrays for Artificial Retinal Implants. *Sensors.* 2008;8:5845-5856.

[19] Loeb GE, Byers CL, Rebscher SJ, et al. Design and fabrication of an experimental cochlear prosthesis. *Med & Biol Eng & Comput*. 1983;21:241-254.

[20] Dorman MF, Smith LM, Dankowski K, et al. Long-Term Measures of Electrode

Impedance and Auditory Thresholds for the Ineraid Cochlear Implant. *J Speech Hear Res*. 1992;35:1126-1130.

[21] Li L, Parkins CW, Webster DB. Does electrical stimulation of deaf cochleae prevent spiral ganglion degeneration?. *Hear Res*. 1999;133:27-39.

[22] Cui X, Wiler J, Dzaman M, et al. In vivo studies of polypyrrole/peptide coated neural probes. *Biomaterials*. 2003;24:777-787.

Figure Legends

Figure 1. (a) Representative schematic of LCP based microelectrode array fabrication process. Laser machining was utilized for patterning the substrate and cover films, and for cutting the electrode array outlines. Thermal-press bonding was performed to create the LCP multi-layered structure. Total thickness of the structure is controllable from 50 to 75 µm with a 25 µm-thick additional substrate. (b) Schematic diagram of LCP based retinal electrode array. This structure has 7 stimulation sites and 1 reference site. The diameters of the stimulation site and reference site windows are 500 µm and 1400 µm, respectively.

Figure 2. *In vitro* reliability tests: (a) schematic diagram of electrode site impedance measurement apparatus, (b) schematic diagram of electrode site arrangement showing channel numbers 1-4 and the reference electrode, (c) cross sectional diagram showing layers in the blister test samples for determination of adhesion strength between LCP/LCP and Ti/LCP interfaces, (d) photographs of samples for blister testing, (e) conceptual diagram of soak and blister testing process, and (f) photograph of blister test apparatus.

Figure 3. Photographs of LCP based Au microelectrode array: (a) FE-SEM image of microelectrode array (Top view) and (b) oblique view of a portion of the array edge, (c) 500 µm diameter Au site and (d) a portion of the Au site window edge. Laser machined site windows and structure outlines exhibited clear, smooth, and rounded edge features. (e) a photograph of the overall structure.

Figure 4. Electrode site impedance monitoring data: (a) magnitude of impedance of Au electrodes on LCP under 37ºC PBS soak test, and (b) magnitude of impedance at 75ºC. The electrode impedance showed initial drop before reaching steady values. The impedance from the 75°C soak stabilized more quickly than that from the 37°C soak. After the stabilization period, the impedance of each of the electrode sites was maintained over the 8 weeks and there was no marked differences between the soak test results from the two soak temperatures.

Figure 5. Blister test results: (a) initial adhesion strengths without soaking, (b) adhesion of LCP/LCP and Ti/LCP interfaces under 37ºC PBS soak test, (c) adhesion of LCP/LCP and PI/PI interfaces under 75ºC PBS soak test, and (d) adhesion of Ti/LCP and Ti/PI

interfaces under 75ºC PBS soak test. The measurement limit (1.1 MPa) was the upper limit of applied pressure in the test apparatus. Error bars represent ±1 standard error (N = 5). The data show that the LCP/LCP and Ti/LCP interfaces were stronger and more reliable than the PI/PI and Ti/PI interfaces during the 8 week soak test.

Figure 6. EECPs recording: (a) Representative EECP waveforms measured in visual cortex of a rabbit, (b) relationship between stimulation intensity and the first positive peak amplitude. The first positive peak (P1) was clearly observed and its implicit time was 26 ms. And, P1 had a nearly linear relationship with the stimulation amplitude.

Figure 7. Suprachoroidally implanted microelectrode array in the rabbit eye: (a) OCT image – 2 weeks post-operation, (b) OCT image - 12 weeks post-operation. (c) fundus image - immediately after operation, (d) fundus image 7 weeks post-operation, (e) histology of the retina – 16 weeks post operation (* indicates the space where the microelectrode array was implanted), (f) FE-SEM image of the microelectrode array explanted after 16 weeks. The retina structures with LCP based microelectrode array were well preserved at the end of the 4 month period. No migration or deformation of the implanted array was found.